

## Optimizing Water Exchange Rates and Rotational Mobility for High-Relaxivity of a Novel Gd-DO3A Derivative Complex Conjugated to Inulin as Macromolecular Contrast Agents for MRI

Luigi Granato,<sup>1</sup> Luce Vander Elst,<sup>1</sup> Celine Henoumont,<sup>1</sup> Robert N. Muller,<sup>1,2</sup> Sophie Laurent<sup>1,2</sup>

<sup>1</sup> General, Organic and Biomedical Chemistry Unit, NMR and Molecular Imaging Laboratory,

University of Mons, Avenue Maistriau, 19, B-7000 Mons, Belgium

<sup>2</sup> Center for Microscopy and Molecular Imaging (CMMI), Rue A. Bolland, 8, 6041 Gosselies, Belgium

Corresponding author mail id: sophie.laurent@umons.ac.be

### Abstract

Thanks to the understanding of the relationships between the residence lifetime  $\tau_M$  of the coordinated water molecules to macrocyclic Gd-complexes and the rotational mobility  $\tau_R$  of these structures, and according to the theory for paramagnetic relaxation, it is now possible to design macromolecular contrast agents with enhanced relaxivities by optimizing these two parameters through ligand structural modification. We succeeded in accelerating the water exchange rate by inducing steric compression around the water binding site, and by removing the amide function from the DOTA-AA ligand [1,4,7,10-tetraazacyclododecane-1,4,7,10-tetraacetic acid mono(p-aminoanilide)] (**L**) previously designed. This new ligand 10[2(1-oxo-1-p-propylthioureidophenyl-propyl)-1,4,7,10-tetraazacyclododecane-1,4,7-tetraacetic acid (**L<sub>1</sub>**) was then covalently conjugated to API [O-(aminopropyl)inulin] to get the complex API-(GdL<sub>1</sub>)<sub>x</sub> with intent to slow down the rotational correlation time ( $\tau_R$ ) of the macromolecular complex. The

This article has been accepted for publication and undergone full peer review but has not been through the copyediting, typesetting, pagination and proofreading process, which may lead to differences between this version and the Version of Record. Please cite this article as doi: 10.1002/cbdv.201700487

This article is protected by copyright. All rights reserved.

evaluation of the longitudinal relaxivity at different magnetic fields and the study of the  $^{17}\text{O}$  NMR at variable temperature of the low-molecular-weight compound ( $\text{GdL}_1$ ) showed a slight decrease of the  $\tau_{\text{M}}$  value ( $\tau_{\text{M}}^{310}=331\text{ns}$  vs  $\tau_{\text{M}}^{310}=450\text{ns}$  for the  $\text{GdL}$  complex). Consequently to the increase of the size of the  $\text{API-(GdL}_1\text{)}_x$  complex, the rotational correlation time becomes about 360 times longer compared to the monomeric  $\text{GdL}_1$  complex ( $\tau_{\text{R}} = 33700\text{ps}$ ), which results in an enhanced proton relaxivity.

## Keywords

Contrast agents, Gd complexes, relaxivity, MRI, NMRD profiles

## Introduction

Magnetic Resonance Imaging (MRI) has become an important technique in modern diagnostic medicine, providing high-quality three-dimensional images of soft tissue without the need for harmful ionizing radiation.<sup>[1]</sup> The difference in signal intensity between tissues or anatomic spaces can be enhanced by manipulation of imaging parameters and/or by the introduction of certain chemical (contrast) agents that influence the relaxation of water, the most abundant substance in human tissues. These contrast agents (CAs) are paramagnetic compounds that shorten the relaxation times of local proton spins ( $T_1$  and  $T_2$ ) and result in an increase of the signal intensity of  $T_1$ -weighted images and decrease it in  $T_2$ -weighted images.<sup>[2]</sup>

The majority of the approved CAs are gadolinium chelates that are based both on macrocyclic tetraazapolyaminocarboxylate chelators (e.g., Dotarem<sup>®</sup>, Prohance<sup>®</sup>, and Gadovist<sup>®</sup>) or open-chain polyaminocarboxylate chelators (e.g., Magnevist<sup>®</sup>, Omniscan<sup>®</sup>, and Multihance<sup>®</sup>).

These low-molecular-weight chelates constitute the first generation of MRI contrast agents and are extracellular fluid agents as they equilibrate rapidly between the intravascular and interstitial space and do not interact specifically with any type of cells.<sup>[3]</sup>

The efficiency of such contrast agents is evaluated on the basis of their relaxivity, or how much the relaxation rates of water protons are increased in the presence of the

agent at a given concentration. The observed relaxation rates of solvent protons result from both paramagnetic ( $1/T_{1,p}$ ) and diamagnetic ( $1/T_{1,d}$ ) contributions. The paramagnetic contribution is linearly related to the concentration of paramagnetic species present, while the diamagnetic contribution corresponds to the relaxation rate of the solvent (water) nuclei in the absence of a paramagnetic solute. The overall relaxivity ( $r_1$ ) of the water nuclei observed in aqueous solution of paramagnetic  $Gd^{3+}$ -complexes is governed mainly by two mechanisms: an inner-sphere component from the proton relaxation of a solvent molecule directly coordinated to the  $Gd^{3+}$  ion, and an outer-sphere component from bulk solvent.<sup>[4-6]</sup> Current agent design focuses mainly on attaining higher inner-sphere longitudinal relaxivity,  $r_1^{is}$ , from protons of water molecules in the first coordination sphere of the metal. Equation 1 reveals that if water exchange at the  $Gd^{3+}$  center is fast enough (small values of  $\tau_M$ , the mean water residence time), the paramagnetic relaxation enhancement experienced by the bulk solvent will come from the relaxation rate ( $1/T_{1M}$ ) increase of the coordinated solvent molecule ( $1/T_1$  is the longitudinal relaxation rate,  $q$  is the number of bound solvent molecules, and  $P_M = [Gd]/55.6$ , is the mole fraction of water coordinated to the metal center). According to the Solomon-Bloembergen-Morgan (SBM) equations of paramagnetic relaxation theory,<sup>[7-9]</sup>  $T_{1M}$  for the dipole-dipole relaxation mechanism is defined by Equation 2. This equation shows that modulation of the correlation time  $\tau_c$  defined in Equation 3 (where  $1/T_{ie}$  is the electronic longitudinal and transverse relaxation rate) becomes critical in the obtainment of the high relaxivities predicted by theory.<sup>[4,6]</sup>

$$r_1^{is} = \frac{1}{T_1} = \frac{q \cdot P_M}{(T_{1M} + \tau_M)} \quad \text{Eq. 1}$$

$$\frac{1}{T_{1M}^{dip}} = \frac{2}{15} \left( \frac{\mu_0}{4\pi} \right)^2 \frac{\gamma_I^2 g^2 S(S+1) \beta^2}{r_{Gd-H}^6} \left[ \frac{3\tau_{c1}}{1 + \omega_H^2 \tau_{c1}^2} + \frac{7\tau_{c2}}{1 + \omega_S^2 \tau_{c2}^2} \right] \quad \text{Eq. 2}$$

$$\frac{1}{\tau_{ci}} = \frac{1}{\tau_R} + \frac{1}{\tau_M} + \frac{1}{T_{ie}} \quad (i = 1, 2) \quad \text{Eq. 3}$$

The relaxivities of current commercial agents based on polyaminocarboxylate scaffolds are small compared to what is theoretically possible, with  $r_1$  values of only 4-5  $\text{mM}^{-1} \text{s}^{-1}$  at 20 MHz. By virtue of these equations 1-3, scientists have focused on

maximizing the hydration number  $q$  ( $q = 1$  for all commercial agents), on optimizing  $\tau_M$  (150-1000 ns in commercial agents), and the rotational correlation time  $\tau_R$  (in the ps regime for small molecules) in order to increase the relaxivity.<sup>[10]</sup> It has indeed been demonstrated that for small-molecular-weight  $Gd^{3+}$ -complexes with optimized  $\tau_M$ , the overall relaxivity is mainly controlled by the rotational correlation time. Figure 1 depicts simulations of relaxivity profiles at several values of rotational correlation time  $\tau_R$  and water residence time  $\tau_M$  with fixed values of electronic parameters.<sup>[11]</sup> It is clear that every magnetic field requires different optimal parameters of  $\tau_R$  and  $\tau_M$  and the maximum relaxivity can be achieved at fields corresponding to the proton Larmor frequency 10-70 MHz (magnetic field 0.24-1.65 T) with  $\tau_R$  as high as possible and  $\tau_M$  in the range 10-50 ns.

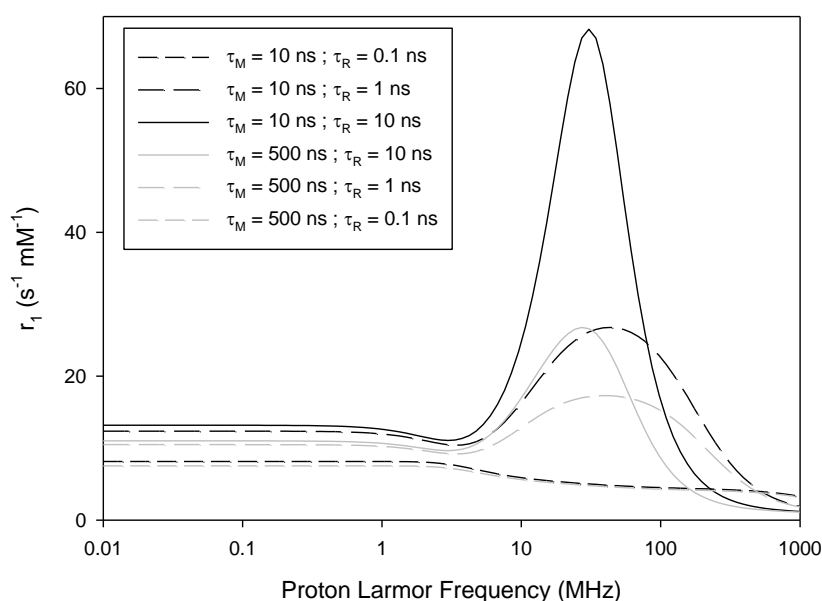


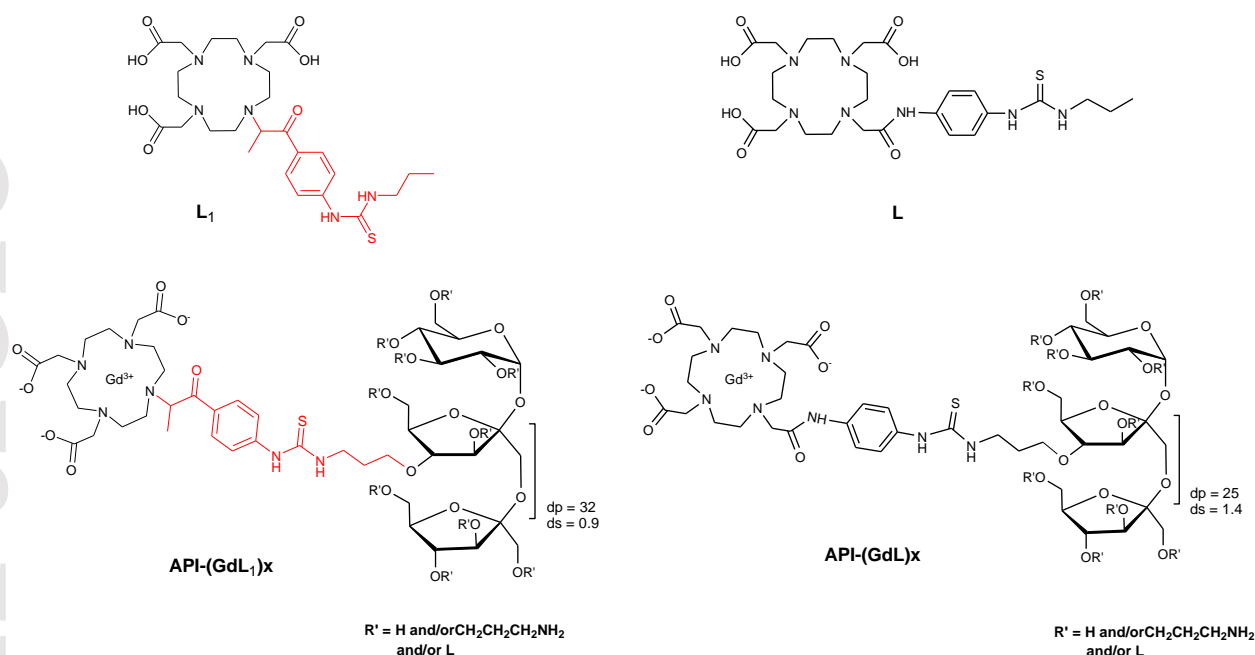
**Figure 1** Simulations of relaxivity as a function of proton Larmor frequency ( $^1H$  NMRD profile) with  $^{298}\tau_M = 10$  ns (black) and 500 ns (grey) and  $^{298}\tau_R = 100$  ps, 1 ns and 10 ns.  $T = 37$  °C,  $^{298}\tau_v = 40$  ps,  $R_{GdH} = 3.1$  Å. Adapted from [11]

A different situation takes place at higher frequencies 100-400 MHz (fields 2.35-9.4 T) where a shorter  $\tau_M$  is more suitable and  $\tau_R$  should have an intermediate value. In the design of  $Gd^{3+}$ -based CAs, this should be taken into account. In particular, optimal values of about 1-30 ns for water residence times ( $\tau_M$ ; optimal value decreases with increasing magnetic field strength) and ns values of the rotational correlation time ( $\tau_R$ )

are required to reach the peak in the relaxivity profile. It is therefore necessary to increase water exchange rates and slow down molecular tumbling relative to commercial agents, while also maintaining long electronic relaxation times with a high number of inner-sphere water molecules to achieve the high relaxivities predicted by theory. Although attaining a more favorable combination of these parameters relative to current agents is desirable, it must come without sacrificing chelate stability, so that toxicity due to free  $\text{Gd}^{3+}$  is avoided.

The aim of this article is to demonstrate how to enhance the relaxivity at 1.5 T (the most common magnetic field used in MRI scanner) of the  $\text{Gd}^{3+}$ -complexes by modulating only the  $\tau_{\text{M}}$ , and/or  $\tau_{\text{R}}$ , while the number of coordinated water molecules ( $q$ ) stays constant. As previously demonstrated<sup>[6]</sup>, the increase of  $q$  leads always to complexes characterized by a lower stability due to the reduced coordination number with gadolinium. As a consequence, only stable  $\text{Gd}^{3+}$ -complexes of macrocyclic DO3A-derivatives, that have one inner-sphere water molecule directly coordinated to the paramagnetic centre, will be studied.<sup>[6]</sup>

The work is divided in two parts: a small monomeric Gd-complex ( $\text{GdL1}$ , scheme 1) will first be synthesized by modifying a Gd-complex previously published ( $\text{GdL}$ )<sup>[12]</sup> in order to optimize the  $\tau_{\text{M}}$  value. It will secondly be covalently attached to inulin ( $\text{API-(GdL)}_x$ , scheme 1) to achieve an optimal value of the  $\tau_{\text{R}}$  at around 10 ns at 1.5 T and again be compared to a previously synthesised macrocyclic Gd-complex ( $\text{API-(GdL)}_x$ ).<sup>[12]</sup> Inulin is a polydisperse polysaccharide which consists of  $\beta(2\rightarrow1)$  fructosyl fructose units with one glucopyranose unit at the reducing end. Depending on the source, the degree of polymerization ( $dp$ ) of inulin varies from 10 to 30. This leads to an average molecular weight distribution in a range between 1.5 and 5 kDa, which is favourable for the preparation of macromolecular conjugates : it allows an increase of the  $\tau_{\text{R}}$  of the Gd-complex as well as an increase of the  $\text{Gd}^{3+}$  concentration per molecule, which should be accompanied by an increase of the relaxivity of the compound.<sup>[13]</sup> Furthermore, inulin and its derivatives possess a low viscosity in aqueous solutions and do not metabolize in blood; both properties can be considered as advantageous for the application of MRI CAs.



**Scheme 1** : Representation of the Gd-complexes with the chemical structural difference between ligand  $L_1$  and  $L$  previously published.<sup>[12]</sup>

## Results and Discussion

### 1. Synthesis and relaxometric characterization of the $\text{GdL}_1$ complex : optimizing the water residence time $\tau_M$ .

The rate of exchange between the water molecule coordinated to a metal ion and bulk water is quite important in the design of most efficient CA for MRI.<sup>[14]</sup> SBM theory predicts that for a  $\text{Gd}^{3+}$ -based  $T_1$  agent to achieve its highest  $T_1$  sensitivity (maximum  $r_1$ ), the optimal bound water lifetime is about 10 ns at 1.5T.<sup>[6]</sup> Various strategies to modify  $\tau_M$  have been discussed in the literature<sup>[15]</sup> but for the purpose of this work, we will briefly describe those factors that can be manipulated on a chemical basis by ligand design. These effects can generally be attributed to stabilization or destabilization of intermediates involved in the water exchange mechanism and/or changes in the population of various CA isomers present in solution.

One of the strategies to increase the rate of water exchange is to modulate the steric hindrance around the  $\text{Gd}^{3+}$  coordination sphere which forces the bound water molecule to reside, on average, further away from the  $\text{Gd}^{3+}$ -ion, thereby making it easier for the water molecule to leave the coordination sphere and mix with the much

larger pool of bulk water molecules. This has been demonstrated by a comparison of the water exchange rate in the  $\text{Gd}^{3+}$ -complexes of DOTA (macrocycle containing 12 atoms,  $\tau_M = 122$  ns) with TRITA (macrocycle containing 13 atoms,  $\tau_M = 3.7$  ns)<sup>[16]</sup> or DO3A-N-prop (one acetate replaced by a propionate,  $\tau_M = 16.4$  ns)<sup>[17]</sup> (see Figure 2a to inspect the ligand structures discussed in this section). While Gd-DO3A-N-prop displays a near optimal  $\tau_M$  value, the kinetic stability of the complex is somewhat compromised compared with Gd-DOTA. This effect is even more pronounced in Gd-TRITA, which has a relatively poor kinetic stability ( $k_1 = 0.21 \text{ M}^{-1}\text{s}^{-1}$ ).<sup>[18]</sup> Adding a charged group to the ligand also has an effect on water exchange. For example, addition of an amino group to the propyl sidechain of DO3A-N-prop to yield DO3A- $\alpha$ -amino-prop results in a dramatic shortening of the bound water lifetime (25 ns) in comparison with the Gd-DOTA complex.<sup>[19]</sup> On the other hand, when a negatively charged acetate group is added to DO3A-N-prop to form DOTA-SA, the water exchange rate in the corresponding  $\text{Gd}^{3+}$ -complex becomes slower ( $\tau_M = 159$  ns)<sup>[20]</sup> compared to the DO3A- $\alpha$ -amino-prop derivative. An interesting feature of the Gd-DOTA-SA complex is that its rotational correlation time is larger than for Gd-DOTA (125 ps versus 53 ps, respectively) which must be attributed to the additional negative charge of the extra carboxylate. It is believed that this carboxylate may assemble extra water molecules in the second coordination sphere which makes the effective molecular weight of the complex larger and hence molecular rotation becomes slower. Gd-DOTA-SA also has the highest thermodynamic stability ( $\log K_{\text{st}} = 27.2$ ) reported to date for DOTA-like complexes and this again can be attributed to the excess negative charge.<sup>[20]</sup> Addition of a bulky group onto the  $\alpha$ -position of an acetate sidechain also has an impact on water exchange. For example, when four methyl groups are introduced, one per acetate, as in Gd-DOTMA, the population of coordination isomers changes from favouring the SAP isomer in Gd-DOTA to preferring the TSAP isomer in Gd-DOTMA.<sup>[21]</sup> Given that water exchange has been observed to be ~50-fold faster in TSAP isomers compared with SAP isomers (Fig. 2 b), it is not surprising to find that the measured water exchange lifetime is faster in Gd-DOTMA ( $\tau_M^{310} = 85$  ns) than in Gd-DOTA ( $\tau_M^{310} = 122$  ns).

Another way to modulate the  $\tau_M$  is to replace the negatively carboxylate groups ( $-\text{COO}^-$ ) with neutral amide groups ( $-\text{CONHR}$ ) which is one effective way to slow the water exchange rate in DOTA-based complexes. Given that the oxygen atom of an amide group is less basic than an oxygen atom of carboxylate, a single amide

substitution can have a dramatic effect on the rate of water exchange. For example, water exchange in the mono-amide complex, Gd-DOTA-1-Bz-NO<sub>2</sub>, is about 5-fold slower ( $\tau_M = 625$  ns) than that in Gd-DOTA. Typical Gd-DOTA-bis-amide complexes display even slower water exchange as evidenced by the  $\tau_M$  value reported for Gd-DOTA-2DMA (811 ns)<sup>[22]</sup> while Gd-DOTA-tetra-amide complexes such as Gd-DOTAM have bound water lifetimes extending into the several  $\mu$ s range (19  $\mu$ s).<sup>[23]</sup> It has also been shown that the bound water lifetime decreases with an increase in the number of methyl substituents on the amide nitrogen (compare Gd-DTMA [ $\tau_M = 17$   $\mu$ s] versus Gd-DOTTA [ $\tau_M = 7.8$   $\mu$ s]).<sup>[23]</sup>

This indicates that the increased steric bulkiness provided by the two methyl substituents can be used to fine-tune water exchange rates in such complexes.



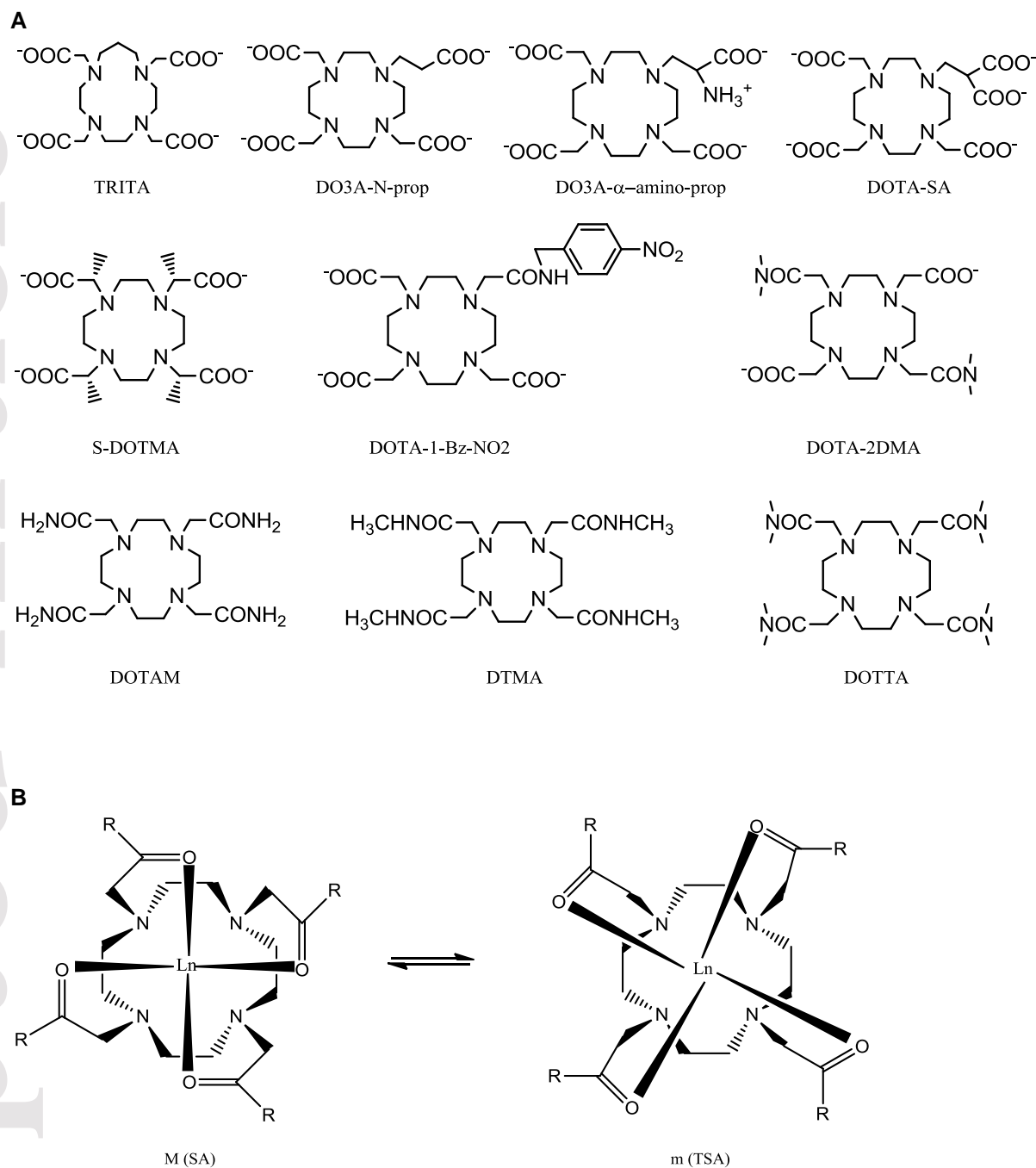
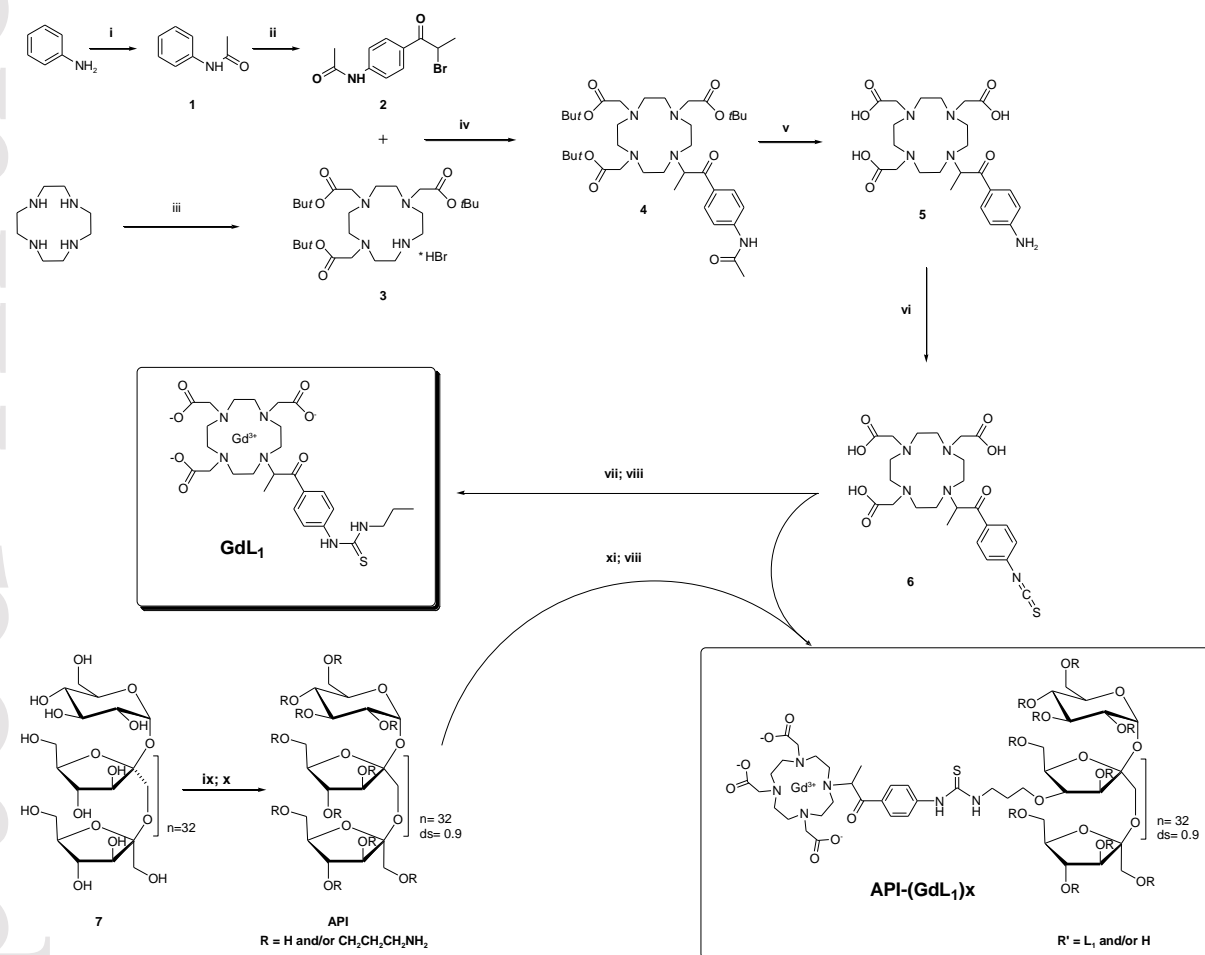


**Figure 2** (a) Structures of some DOTA-based ligands discussed in this section; (b) two diastereoisomeric forms, *M* (SA) and *m* (TSA), of Ln (III) complexes with DOTA-type ligands. Adapted from [6]

On the basis of these observations, we set off with the idea of inducing steric compression around the water binding site in dissociatively exchanging Gd<sup>3+</sup>-complex by adding a methyl group (-CH<sub>3</sub>), and by removing the neutral amide groups (-CONHR) from the DOTA-derivative ligand (**L**), previously synthesised and described elsewhere (Scheme 1),<sup>[12]</sup> in order to accelerate the water exchange without decreasing its well-known complex stability.

The new complex **GdL<sub>1</sub>** was obtained by following the reactions outlined in Scheme 2. This route required the synthesis of a particular linker (**2**), which is later added to the 1,4,7,10-tetraazacyclodecane-1,4,7-tris-(acetic acid *t*-butyl ester) (**3** DO3A-*t*Bu), by using the same alkylation condition employed in the previously published synthesis.<sup>[12]</sup>



**Scheme 2** Synthesis of **API-(GdL<sub>1</sub>)<sub>x</sub>** and **GdL<sub>1</sub>**: (i) acetyl chloride, K<sub>2</sub>CO<sub>3</sub>, CH<sub>2</sub>Cl<sub>2</sub>, 0 °C; (ii) Bromopropionyl bromide, 1,2,4-trichlorobenzene, AlCl<sub>3</sub>, 70 °C; (iii) *tert*-butyl bromoacetate, NaHCO<sub>2</sub>, CH<sub>3</sub>CN; K<sub>2</sub>CO<sub>3</sub>, CH<sub>3</sub>CN; (iv) K<sub>2</sub>CO<sub>3</sub>, CH<sub>3</sub>CN, room temperature (rt); (v) 0.1 M HCl, CH<sub>3</sub>CN, 100 °C, 4h; (vi) CSCI<sub>2</sub>, CCl<sub>4</sub>/water, rt; (vii) water, 1-propylamine, pH 9-10; (viii) GdCl<sub>3</sub>·6H<sub>2</sub>O, pH 6.5-7.0; (ix) acrylonitrile, aqueous NaOH, 45 °C; (x) Li, liquid NH<sub>3</sub>; EtOH, 50 °C; (xi) water, pH 9-10, room temperature.

The preparation of the 4-acetamido- $\alpha$ -bromopropiophenone (**2**) was attempted by using of conventional Friedel-Crafts conditions, where bromopropionyl bromide was added at 70 °C in a pre-incubated mixture of acetanilide and aluminium trichloride, in 1,2,4-trichlorobenzene as a solvent.

The final **GdL<sub>1</sub>** complex was obtained via the same complexation method previously described for synthesising the agent **GdL**.<sup>[12]</sup>

### Variable-temperature <sup>17</sup>O NMR measurements

The determination of the water exchange rate  $k_{\text{ex}}$  (or the residence lifetime of water molecule in the first coordination sphere  $\tau_M = 1/k_{\text{ex}}$ ) is of utmost importance. This parameter contributes directly to the modulation of the electron-nuclear dipolar interaction as it controls the efficiency of the transfer of the paramagnetic effect to the bulk water. The water exchange rate of **GdL<sub>1</sub>** was determined from a variable temperature <sup>17</sup>O NMR study, more specifically from the temperature dependence of the transverse relaxation rate  $1/T_2$  of the water in an aqueous solution of the compound of interest (figure 3a).

The experimental data were fitted with a theoretical model as described previously,<sup>[24]</sup> which gives a  $\tau_M^{310}$  value of  $331 \pm 44$  ns. This is lower than that calculated for **GdL** ( $450 \pm 20$  ns), but higher than that for Gd-DOTA ( $122 \pm 10$  ns) complex. A detailed discussion of these calculated results is presented in the next paragraph, where the Nuclear Magnetic Relaxation Dispersion (NMRD) data are discussed.

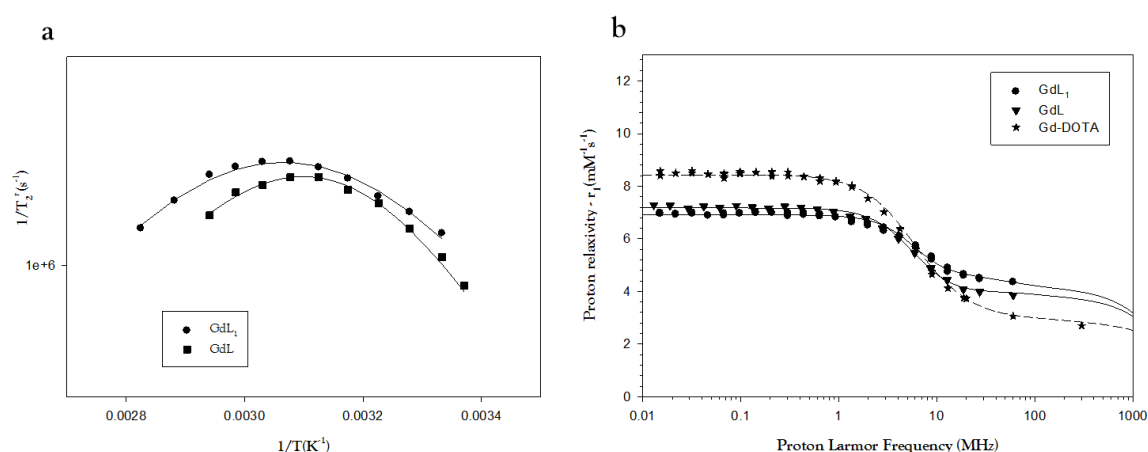


**Figure 3** (a) Temperature dependence of the reduced <sup>17</sup>O transverse relaxation rate at 11.75 T; (b) comparison between <sup>1</sup>H NMRD profiles of **GdL<sub>1</sub>** 1.78 mM (spheres), **GdL** 2.60 mM (triangles) and Gd-DOTA (stars). The lines represent simulation using the best-fit parameters (Table 1).

### Simultaneous Fitting of NMRD and <sup>17</sup>O NMR Data

In the NMRD studies, the longitudinal proton relaxation rate enhancements are generally expressed in terms of the relaxivity  $r_1$  (mM<sup>-1</sup> s<sup>-1</sup>). The observed

paramagnetic relaxation results from a sum of contribution originating from short-distance interactions (inner-sphere mechanism) and from longer-distance interactions (outer-sphere mechanism). The influence of  $\tau_M$  on proton relaxivity is well understood. When this exchange time is short relative to the relaxation time of the protons of the coordinated water molecules, the overall proton relaxivity is enhanced by a temperature decrease. On the contrary, when the exchange time is long, the global relaxivity is levelled off or even decreased by a reduction of the temperature.

The fittings of the proton NMRD profiles were performed as described in the experimental section according to the classical paramagnetic relaxation formalisms.<sup>[7,25,26]</sup> The following strategy was adopted: after subtraction of the diamagnetic relaxation rate of the solvent, the outer-sphere and the inner-sphere contributions were simultaneously fitted after attribution of fixed or calculated values to the various parameters. The relative diffusion constant  $D$  was fixed to the diffusion constant of water ( $D = 3 \times 10^{-9} \text{ m}^2 \text{ s}^{-1}$ ),  $d$ , the distance of closest approach for the outer sphere contribution was set at 0.36 nm,  $\tau_M$  values were those obtained by  $^{17}\text{O}$  NMR and  $q$ , the number of water molecules in the first coordination sphere of  $\text{Gd}^{3+}$ , was given a value of one. The parameters describing the electronic relaxation times,  $\tau_v$  and  $\tau_{s0}$  (the electronic relaxation time at zero field), and the rotational correlation time ( $\tau_R$ ) were optimized for the outer-sphere and the inner-sphere contributions simultaneously. The structure of the complex  $\text{GdL}_1$  as well as the shape of its NMRD profile do not justify in this case the introduction of a second sphere contribution.

The parameters obtained from the fitting are listed in Table 1 with the curve fits shown in Figure 3b. For comparison, previously published data for **GdL** and Gd-DOTA have been included in the Table 1.<sup>[12,27]</sup> It can be noted that the relaxivities measured for the three complexes are all in the same range. In particular, the  $r_1$  of **GdL**<sub>1</sub>, measured at 20 MHz and 310 K, is  $4.7 \text{ mM}^{-1} \text{ s}^{-1}$ . This value is slightly higher than that of the **GdL** complex previously calculated ( $r_1 = 4.2 \text{ mM}^{-1} \text{ s}^{-1}$ ),<sup>[12]</sup> and also higher compared to the relaxivity of the Gd-DOTA complex taken as reference ( $3.5 \text{ mM}^{-1} \text{ s}^{-1}$ ).<sup>[27]</sup>

**Table 1** Parameters of **GdL<sub>1</sub>**, and **GdL** obtained from the analysis of <sup>1</sup>H NMRD data compared with Gd-DOTA as a reference.

Parameters	GdL <sup>[11]</sup>	Gd-DOTA	GdL <sub>1</sub>
$\tau_V^{310}$ (ps)	10.5 ± 1.0 (18) <sup>a</sup>	7 ± 1.0	19.2±1.1 (23.8) <sup>a</sup>
$\tau_M^{310}$ (ns)	450 ± 20 <sup>b</sup>	122 ± 10 <sup>b</sup>	331 ± 44 <sup>b</sup>
$\tau_R^{310}$ (ps)	84 ± 3.4	53 ± 1.3	93.1 ± 2.2
$\tau_{SO}^{310}$ (ps)	92.5 ± 3.2	404 ± 24	74.8 ± 1.2

(a) The first values were obtained from the fitting of the proton NMRD profile; the values in parentheses were obtained from the fitting of the <sup>17</sup>O NMR data.

(b) The  $\tau_M$  values are those obtained from the fitting of the <sup>17</sup>O NMR data.

As mentioned above there is a small difference between the values of  $\tau_M$  obtained by <sup>17</sup>O NMR measurement for the two Gd<sup>3+</sup> complexes. Both the rate and the mechanism of the water exchange are intimately related to the structure of the complexes in solution. The steric constrain of the methyl group present on the linkage arm of the **GdL<sub>1</sub>** complex explains a steric compression of these atoms around the site occupied by the water molecule in the first coordination sphere. This destabilizes the bound water molecule and accelerates the water exchange. The increase of the water exchange rate observed for **GdL<sub>1</sub>** complex can also be explained through the replacement of the amide moiety by an oxo-group. The explanation of this structural behaviour is reported in the literature for macrocyclic complexes when one carboxylate of DOTA is substituted by an amide or OH coordination group. An amide group is less strongly coordinated towards the lanthanide ion than a carboxylate, which is exhibited by smaller stability constants of the amide complexes compared to carboxylates in solution,<sup>[28-30]</sup> and by longer Gd-amide oxygen distances in the solid state, when compared to Gd-carboxylate oxygen distances.<sup>[31]</sup> As a consequence, the inner-sphere is less crowded in amide than in carboxylate complexes. In dissociatively activated water exchange processes the steric crowding is of primary importance, that is a tightly coordinating ligand pushes the water molecule to leave, and thus favours the dissociative activation step.<sup>[6]</sup>

The value of the rotational correlation time ( $\tau_R^{310}$ ) follows the general trend of the relative molecular mass of the typical DOTA derivative complexes.<sup>[6]</sup> The higher  $\tau_R$  value for the new complex may be explained through an increased rigidity of the

molecular structure acquired after the modification of the ligand **L<sub>1</sub>** via the replacement of the amide bound.

As expected, the  $\tau_{s0}$  value of **GdL<sub>1</sub>** complex is lower than that of Gd-DOTA. It is usually assumed that the large value of  $\tau_{s0}$  of Gd-DOTA is related to the rigidity and/or the symmetry of the complex. Since **GdL<sub>1</sub>** complex is expected to be less rigid and non-symmetric, its  $\tau_{s0}$  value is lower and comparable to that of **GdL**.

### Kinetic stability of the new monomeric **GdL<sub>1</sub>** complex

It has been demonstrated that gadolinium chelates could be sensitive to transmetallation by endogenous ions such as  $\text{Cu}^{2+}$ ,  $\text{Ca}^{2+}$ , and  $\text{Zn}^{2+}$ .<sup>[48-49]</sup> Only zinc can displace significant amount of  $\text{Gd}^{3+}$  because its concentration in the blood is relatively high (55-125 mol/L), whereas copper is present in very small amount (1-10 mol/L) and calcium ions have low affinity to organic ligands. Transmetallation between  $\text{Gd}^{3+}$  and zinc will result in the formation of zinc chelate which is excreted in urine, while the released  $\text{Gd}^{3+}$  becomes attached to endogenous anions such as phosphate, citrate, hydroxide or carbonate and deposit in tissues as insoluble toxic compounds. For these reasons we investigated the kinetic stability of this new monomeric **GdL<sub>1</sub>** complex by a relaxometric study of its transmetallation with  $\text{ZnCl}_2$ .

The technique is performed by measuring the evolution of the water proton paramagnetic longitudinal relaxation rate ( $R_1^p$ ) of a phosphate buffer solution (pH = 7) containing **GdL<sub>1</sub>** complex and  $\text{ZnCl}_2$  at equal concentration (2.5 mmol/L). The  $R_1^p$  relaxation rate is obtained after subtraction of the diamagnetic contribution of the proton water relaxation ( $0.2826 \text{ s}^{-1}$ ) from the observed relaxation rate  $R_1 = (1/T_1)$ . Upon transmetallation of a paramagnetic  $\text{Gd}^{3+}$  ion by a diamagnetic  $\text{Zn}^{2+}$  ion in phosphate buffer, the released  $\text{Gd}^{3+}$  precipitates as  $\text{GdPO}_4$ , which does not contribute to the relaxivity. Therefore, the overall relaxivity of the solution decreases over time with a rate depending on the rate of transmetallation. This decrease in relaxivity is a good estimation of the kinetic stability of the  $\text{Gd}^{3+}$  complexes. The result of this experiment (Fig. 4) shows a very good kinetic stability of  $\text{Gd}^{3+}$  complex **GdL<sub>1</sub>**, similar to the previous **GdL**, as compared with Magnevist, which shows significant decomplexation during the same time period (5 days).

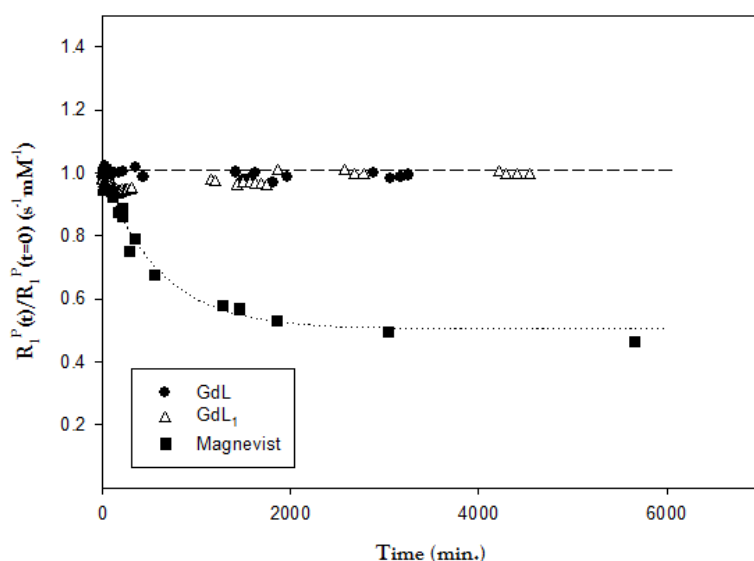


**Figure 4.** Evolution of the water proton paramagnetic longitudinal relaxation rate  $R_1^P(t)/R_1^P(t_0)$  vs time of 2.5mM  $Zn^{2+}$  aqueous solution for **GdL<sub>1</sub>** (2.5mM), **GdL** (2.5mM) and **Magnevist** (2.5mM).

## 2. Conjugation of the Ligand $L_1$ to Inulin: From Small Molecule to Macromolecular Contrast Agents

Small molecular  $Gd^{3+}$ -complexes have a relatively low relaxivity and extravasate non-selectively from blood into the interstitium of both normal tissue and tumor, which has been a major limitation for their clinical applications. As mentioned before, at the magnetic field strengths currently employed in MRI (0.5-1.5 T), the ability of  $Gd^{3+}$ -chelates to enhance the longitudinal water proton relaxation rate is mainly determined by the value of their molecular reorientational time,  $\tau_R$ . Therefore, the achievement of higher water proton relaxation rates may be pursued through an increase of this parameter.

In order to slow down the reorientational motion of  $Gd^{3+}$ -complexes, several techniques have been used. Conceptually, they represent different strategies to increase the effective molecular weight (more precisely, molecular volume) accompanied by an enhancement of  $\tau_R$ . It should be emphasized that the water residence time  $\tau_M$  should be optimized for a particular magnetic field to take full advantage of the increased  $\tau_R$ . Usually, the lengthening of the rotational motion is

pursued through a covalent or noncovalent binding of the paramagnetic complex to macro-/supramolecular carrier. In order to attach paramagnetic ions to larger structures, a class of chelates known as bifunctional chelates have been developed based on DTPA and DOTA. These chelating agents are typically modified to have an electrophilic group that is available for conjugation to nucleophilic groups on biomolecules. For example, these functional groups include anhydride, bromo- or iodo-acetamide, isothiocyanate, *N*-hydroxysuccinimide (NHS) ester and maleimide. In cases where the biomolecules contain only electrophilic functionality, such as a carboxylic acid group, the common strategy is to use cross-linking agents that provide a link between the two moieties or introduce functionality that makes conjugation more amenable.

A vast number of MR macromolecular contrast agents have been reported over the last 30 years, ranging from protein-, to albumin-, polymer-, dendrimer-, carbohydrate-, liposomes-, micelles-based molecules.<sup>[6,12,32-37]</sup> These macromolecular carriers can be linear or of a spherical shape.

The second part of this work will describe the enhancement of the relaxivity  $r_1$ , when the monomer **GdL<sub>1</sub>** complex is conjugated to the inulin as linear carrier. The reasons of choosing the inulin as a biomolecule to synthesize a macromolecular contrast agent were defined in the introduction.

### **Synthesis and relaxometric characterization of the API-(GdL<sub>1</sub>)<sub>x</sub> complex**

The new chelate **L<sub>1</sub>** (Scheme 1) was conjugated to inulin following the synthetic route outlined in Scheme 2. As we know inulin is a polydisperse polysaccharide consisting of  $\beta(2\rightarrow1)$  fructosyl fructose units with one glucopyranose unit at the reducing end. Depending on the source, the degree of polymerization (*dp*) of inulin varies from about 10 to 30. In the present study the *dp* of the polysaccharide used was estimated at 32.

The O-(aminopropyl)inulin (API) was obtained functionalising the inulin through a cyanoethylation by using acrylonitrile and base, followed by reduction of the cyano groups with metallic Li in liquid ammonia-ethanol at low temperature. The theoretical maximum degree of substitution (*ds*) can be three, corresponding to the three available hydroxyl groups per sugar unit in the starting material. However previous



studies have indicated that the cyanoethyl groups in O-cyanoethylinulin are distributed uniformly along the inulin chain and that, within each fructose unit, the 4-position is the most reactive towards cyanoethylation.<sup>[38]</sup>

The final macromolecular ligand **[API-(L<sub>1</sub>)x]** was synthesised by reacting the amino group of the API and the isothiocyanate moiety of the intermediate structure DO3A-NCSP<sup>[6]</sup> (Scheme 2) of ligand **L<sub>1</sub>**. By the study of the <sup>13</sup>C and <sup>1</sup>H NMR spectroscopy of the product **API-(L<sub>1</sub>)x**, an average degree of substitution of 0.9 was obtained.

### Variable-temperature <sup>17</sup>O NMR measurements and NMRD study

The **API-(GdL<sub>1</sub>)x** complex was synthesized in the same way as for the complex GdL<sub>1</sub> already mentioned and described previously. The value of  $\tau_M$  was estimated from the analysis of the temperature dependence of the reduced transverse <sup>17</sup>O relaxation rates, which is almost 2 fold higher than the analog macromolecular complex previously synthesized **[API-(GdL)x]**<sup>[12]</sup> (Scheme 1 and Table 2). For a comparison, Figure 5a shows the <sup>17</sup>O NMR measurements of the two macromolecular complexes, with the theoretical fitting performed as previously described.<sup>[24]</sup>

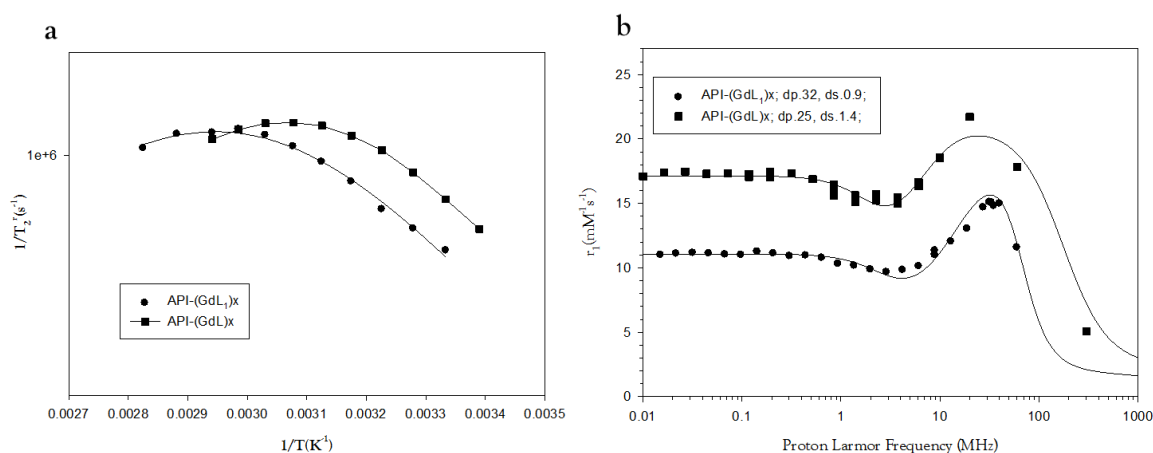


**Figure 5** (a) Temperature dependence of the reduced <sup>17</sup>O transverse relaxation rate at 11.75 T; (b) comparison between <sup>1</sup>H NMRD profiles of **API-(GdL<sub>1</sub>)x** 1.13 mM (spheres), and **API-(GdL)x** 1.18 mM (rectangles). The lines represent simulation using the best-fit parameters (Table 2).

To assess the efficacy of the novel macromolecular contrast agent, **API-(GdL<sub>1</sub>)x**, we measured the longitudinal relaxation rate enhancements of water protons as a function of the Larmor frequency induced by this complex. In Figure 5b, the resulting NMRD profile at 310 K is compared with that of **API-(GdL)x** complex of the corresponding conjugated chelate **L** (Scheme 1). The <sup>1</sup>H NMRD profiles of these

macromolecular complexes were fitted using a model that takes into account inner-sphere, outer-sphere and second-sphere contributions to the paramagnetic relaxation rate. Some parameters were fixed during fitting procedure:  $d$ , the distance of closest approach ( $d = 0.4$  nm when a second sphere contribution is present and  $d = 0.36$  nm in the absence of second sphere contribution);  $D$ , the relative diffusion constant ( $D = 3 \times 10^{-9} \text{ m}^2 \text{ s}^{-1}$ ); and  $r$ , the distance between the  $\text{Gd}^{3+}$  ion and the proton nuclei of water ( $r = 0.31$  nm). The residence lifetime of the inner sphere,  $\tau_M$ , was set to the value determined by  $^{17}\text{O}$  NMR, the distance between  $\text{Gd}^{3+}$  and the protons of the second sphere water molecules,  $r_{ss}$  was fixed at 0.36 nm. The rotational correlation time ( $\tau_R$ ), the electronic relaxation time at zero field ( $\tau_{so}$ ) and its correlation time ( $\tau_v$ ), as well as the number of second-sphere water molecules ( $q_{ss}$ ) and the correlation time modulating the second sphere interaction ( $\tau_{ss}$ ), were treated as adjustable parameters. The conjugation of the paramagnetic complex to the inulin carrier resulted in an increase in  $\tau_R$  (33.7 ns) and consequently in a higher relaxivity comparing to the monomer **GdL<sub>1</sub>** (Table 2). The obtained  $\tau_R$  value is higher than that of the previously synthesized API-(GdL)<sub>x</sub> complex, probably due to the higher degree of polymerization (dp = 32 vs dp = 25) and the increased rigidity of the complex GdL<sub>1</sub> as previously discussed.

**Table 2** Parameters of **API-(GdL<sub>1</sub>)<sub>x</sub>**, **GdL<sub>1</sub>**, **API-(GdL)<sub>x</sub>** and **GdL** obtained from the analysis of  $^{17}\text{O}$  NMR and  $^1\text{H}$  NMRD data compared with Gd-DOTA as a reference.

Parameters	API-(GdL) <sub>x</sub> dp=25; ds=1.4 <sup>[11]</sup>	GdL <sup>[11]</sup>	Gd-DOTA	GdL <sub>1</sub>	API-(GdL <sub>1</sub> ) <sub>x</sub> dp=32; ds=0.9
$r_1^b$ [mM <sup>-1</sup> s <sup>-1</sup> ]	21.7	4.1	3.5	4.7	14.5
$r_1^c$ [mM <sup>-1</sup> s <sup>-1</sup> ]	759.5	4.1	3.5	4.7	417.6
$\tau_v^{310}$ (ps)	45 ± 1.0 (6.2) <sup>a</sup>	10.5 ± 1.0 (18) <sup>a</sup>	7 ± 1.0	19.2 ± 1.1 (23.8) <sup>a</sup>	26.5 ± 0.6 (15.4) <sup>a</sup>
$\tau_M^{310}$ (ns)	625 ± 34	450 ± 20	122 ± 10	331 ± 44	1096 ± 52
$\tau_R^{310}$ (ps)	1460 ± 70.7	84 ± 3.4	53 ± 1.3	93.1 ± 2.2	33700 ± 12.5
$\tau_{so}^{310}$ (ps)	153 ± 7.0	92.5 ± 3.2	404 ± 24	74.8 ± 1.2	105 ± 6.1
$q_{ss}$	5 ± 0.6	c		c	2.10 ± 0.27
$\tau_{ss}$ (ps)	23.4 ± 1.6	c		c	23 ± 2.5

(a) The first values were obtained from the fitting of the proton NMRD profile; the values in parentheses were obtained from the fitting of the  $^{17}\text{O}$  NMR data; (b)  $r_1$  corresponds to the relaxivity per Gd-complex, (c) per

molecule, both calculated at 20 MHz and 37 °C; (c) The structure of the complexes **GdL** and **GdL<sub>1</sub>** as well as the shape of their NMRD profiles do not justify the introduction of a second sphere contribution.

The shape of the NMRD curve of the **API-(GdL<sub>1</sub>)x** complex, particularly the maximum around 20-30 MHz, is characteristic for high-molecular-weight complexes and reflects the effect of the relatively low tumbling time of the complex.

Although the increase of the value of  $\tau_R$  (by increasing the molecular weight of the paramagnetic **API-(GdL<sub>1</sub>)x** complex) causes the increase of total relaxivity, it turns out to be lower than that one measured for the **API-(GdL)x** complex at the same magnetic field strengths (Fig. 5b). One of the reasons to describe this outcome is because the residence lifetime ( $\tau_M$ ) of the inner-sphere water becomes a limiting factor for the relaxivity.

In our particular case, although the water exchange rate measured for the monomer **GdL<sub>1</sub>** complex (Scheme 1) is higher than that of the **GdL** (Scheme 1) due to the reasons above described, the residence lifetime became larger when the **GdL<sub>1</sub>** is conjugate with API. **API-(GdL<sub>1</sub>)x** has indeed a higher degree of polymerisation ( $dp = 32$  vs  $dp = 25$ ), and especially a lower degree of substitution (averaged  $ds = 0.9$  vs  $ds = 1.4$ ) than the macromolecular complex previously reported [**API-(GdL)x**].<sup>[12]</sup> As a consequence, a higher number of -OH groups around the second coordination sphere of the  $Gd^{3+}$  complex limits the access to the water bulk to be coordinated to the paramagnetic centre.

The number of second-sphere water molecules,  $q_{ss}$  obtained from the fitting is lower as compared to the value calculated for **API-(GdL)x** ( $q_{ss} = 2$  vs  $q_{ss} = 5$ ). In summary, the lower relaxivity of **API-(GdL<sub>1</sub>)x** compared to **API-(GdL)x** results from the slower water exchange rate and from a lower number of second sphere water molecules.

## Conclusions

We have reported a similar synthetic pathway for the complexes described previously, with the intent to improve the relaxivity properties of these new complexes by modifying important parameters as  $\tau_M$  and  $\tau_R$ . On the basis of structural considerations in the inner sphere of the monomeric **GdL<sub>1</sub>** complex, we succeeded in accelerating water exchange by inducing steric compression and by removing the

amide group around the water bonding site. The increased steric crowding was achieved by adding a methyl group, whereas the amide group was replaced by an oxo-group from the linker of the DO3A-derivative chelate. Despite these modifications, the kinetic stability of the new complex toward transmetalation with  $\text{Zn}^{2+}$  is not reduced, which is comparable with that of **GdL**, considering also that both macrocyclic structures are very similar.

Analysis of the variable temperature  $^{17}\text{O}$  NMR and NMRD data suggests that the conjugated inulin-based complexes [**API-(GdL<sub>1</sub>)x** and **API-(GdL)x**], having different degree of polymerization ( $dp = 32$  vs  $dp = 25$ ) and different degree of substitution (averaged  $ds = 0.9$  vs  $ds = 1.4$ ), show a dramatic increase in relaxivity for both macromolecular complexes. The substantial increase of the rotational correlation time ( $\tau_R$ ) of the **API-(GdL<sub>1</sub>)x** complex doesn't reflect in the enhancement of its overall relaxivity, because its water exchange rate ( $\tau_M$ ) remains still a limiting factor. As mentioned before, even if the  $\tau_M$  of **GdL<sub>1</sub>** is shorter than that of **GdL**, when the monomeric complex is conjugated to inulin, the efficacy of the macromolecular complex is reduced because of a slowing down of the residence lifetime and a decrease of number of second sphere water molecules.

## Experimental Section

### General methods and materials

All reagents and chemicals were obtained from commercial sources and used without further purification. Solvents were distilled and/or dried prior to use by standard methodology except for those, which were reagent grades. Inulin ( $dp$  32) was donated by Sensus Cooperatie Cosun U.A. (Roosendaal, the Netherlands). The new O-(Aminopropyl)inulin (**API**) was synthesized from inulin by following a procedure described previously.<sup>[38]</sup> Water was demineralized prior to use. Unless stated otherwise, all the reactions were carried out under a nitrogen atmosphere and the reaction flasks were pre-dried by heat gun under vacuum. The pH values of the solution were adjusted using aqueous solution 1M NaOH, 1N pyridine or 1N HCl. Most of the reactions were monitored by TLC on silica plates detecting the components by UV light or by applying the Dragendorff reagent, while other product formations were monitored via analytical HPLC (Waters W600, with a quaternary pump gradient module) with an UV detector coupled with a Waters micromass ZQ

system (Waters, Belgium). For low molecular weight characterization, ESI-QTOF-MS were obtained on a Q-TOF Ultima mass spectrometer (Micromass, Manchester, UK), whereas for high molecular weight products, MALDI spectra were obtained on MALDI-TOF spectrometer (Micromass, Manchester, UK). The purification of the compounds was performed on KP-silica and KP-C18 Biotage cartridges over a Biotage flash chromatography instrument, Uppsala, Sweden. A final purification step of high molecular weight compounds was performed either with a Millipore stirred cell ultra-filtration system using membranes with 0.5, 1, 3 kDa MW cut-off, or via dialysis procedure by using membranes with 150-300 Da MW cut-off.  $^1\text{H}$ -NMR,  $^{13}\text{C}$ -NMR spectra were recorded on either with a Bruker Avance-300 MHz or a Bruker Avance II-500 MHz spectrometer, at 25°C. Chemical shifts are given in ppm ( $\delta$ ) values. Data are reported as follows: chemical shift (multiplicity: s = singlet, d = doublet, t = triplet, q = quadruplet, m = multiplet, br = broad resonance) J = coupling constant (Hz), integration, peak assignment in italic form.

### ***Synthesis of Acetanilide (1)***

To a stirred solution of aniline (10.2 g, 110 mmol) and  $\text{K}_2\text{CO}_3$  (12.9 g, 165 mmol) in  $\text{CH}_2\text{Cl}_2$  at 0 °C, acetyl chloride (7.6 g, 55 mmol) in  $\text{CH}_2\text{Cl}_2$  (volume) was added dropwise after 10 min.

The resulting reaction mixture was stirred at this temperature for a further 4 h, and monitored via TLC with Hexane/EtOAc (7:3) as a mobile phase mixture.

After 24h, the reaction was stopped and poured into water. The aqueous layer was extracted twice with methylene chloride. The organic phase was combined, washed three times with a dilute hydrochloric acid/water solution (pH=2), and dried over  $\text{Na}_2\text{SO}_4$ , and evaporated to dryness to give a pure compound (12.1 g, 81.1% yield) as a pale white solid. ESI MS:  $m/z$  136 [ $\text{M} + \text{H}$ ] $^+$ ;  $^1\text{H}$  NMR (500 MHz,  $\text{CDCl}_3$ , 25 °C, TMS):  $\delta$  2.10 (3H, s,  $\text{CH}_3$ ), 7.02 (1H, t,  $\text{ArH}$ , J = 7Hz), 7.28 (2H, t,  $\text{ArH}$ , J = 7Hz), 7.55 (2H, d,  $\text{ArH}$ , J = 7Hz), 9.75 (1H, s,  $\text{NHCO}$ ).  $^{13}\text{C}$  NMR (500 MHz,  $\text{CDCl}_3$ , 25 °C, TMS):  $\delta$  24.05, 119.97, 123.78, 128.50, 140.32, 169.21.

### ***Synthesis of 4-Acetamido- $\alpha$ -bromopropiophenone (2)***

Bromopropionyl bromide (8.8 g, 41 mmol) was added at 70 °C to a stirred mixture of acetanilide (5.0 g, 37 mmol) and aluminium trichloride (15.0 g, 112 mmol) in 1,2,4-

trichlorobenzene (25 ml) so that the temperature did not exceed 80 °C . The mixture was stirred for a further 30 minutes at 80 °C, cooled to 60 °C and methanol (5 ml) added slowly with cooling to keep the temperature below 70 °C, followed by cautious addition of water (50 ml). On cooling, the product crystallized out of the organic layer and dichloromethane was added to redissolve it. The organic layer was separated, washed with water (twice), aqueous sodium bicarbonate, dried (Na<sub>2</sub>SO<sub>4</sub>), filtered and concentrated at 60 °C. Petroleum ether (60 °C - 80 °C) was then added to crystallise a solid which was collected and dried to give 4-acetamido- $\alpha$ -bromopropiophenone (9.18 g; 91% yield), m.p. 107°C - 112°C. ESI MS:  $m/z$  271-273 [M + H]<sup>+</sup>; <sup>1</sup>H NMR (500 MHz, CDCl<sub>3</sub>, 25 °C, TMS):  $\delta$  1.89-1.90 (3H, d, BrCHCH<sub>3</sub>, J = 7Hz), 2.09 (3H, s, COCH<sub>3</sub>), 5.66 (1H, q, BrCH, J = 10 Hz), 7.68 - 7.97 (5H, 2 d + 1 br s, ArH (J = 8 Hz), NHCO). <sup>13</sup>C NMR (500 MHz, CDCl<sub>3</sub>, 25 °C, TMS):  $\delta$  20.58, 24.18, 42.85, 120.12, 130.56, 131.40, 145.08, 172.00, 194.23.

**Synthesis of 1,4,7,10-tetraazacyclodecane-1,4,7-tris(acetic acid t-butyl ester) hydrobromide salt (3)**

1,4,7,10-Tetraazacyclodecane (10.0 g, 58 mmol) and sodium hydrogen carbonate (16.1 g, 192 mmol) were stirred in freshly distilled acetonitrile (200 ml) cooled to 0 °C under N<sub>2</sub>. Tert-butyl bromoacetate (37.4 g, 192 mmol) was added dropwise over 30 min. After addition, the reaction mixture was allowed to reach ambient temperature and stirred for a further 48 h. The inorganic solids were removed by filtration and the filtrate evaporated under reduced pressure to leave a pale-white solid. The crude solid product was stirred in toluene for 24 h, offering the title ester (**3**) as a white solid (24.36 g, 81.6%). ESI MS:  $m/z$  515 [M + H]<sup>+</sup>,  $m/z$  537 [M + Na]<sup>+</sup>; <sup>1</sup>H NMR (500 MHz, CDCl<sub>3</sub>, 25°C, TMS):  $\delta$  1.47 [27H, s, C(CH<sub>3</sub>)<sub>3</sub>], 2.88-2.94 (12H, br m, CH<sub>2</sub>CH<sub>2</sub>), 3.11 (4H, br s, CH<sub>2</sub>CH<sub>2</sub>), 3.30 (2H, s, NCH<sub>2</sub>COO), 3.38 (4H, s, NCH<sub>2</sub>COO), 10.03 (2H, br s, NH<sub>2</sub>). <sup>13</sup>C NMR (500 MHz, CDCl<sub>3</sub>, 25 °C, TMS):  $\delta$  28.21, 28.25, 47.54, 49.22, 51.38, 58.25, 81.71, 81.87, 169.65, 170.54.

**Synthesis of 10[2(1-oxo-1-p-acetamidophenyl propyl)]-1,4,7,10 tetraaza cyclodecane-1,4,7-tris(acetic acid t-butyl ester) (4)**

Into a two-necked round bottom flask, under dry condition (N<sub>2</sub>), a suspension of 1,4,7,10-tetraazacyclodecane-1,4,7-tris(acetic acid t-butyl ester) hydrobromide salt



(3) (4.64 g, 9.02 mmol) and  $K_2CO_3$  (1.87 g, 13.5 mmol) in HPLC-grade  $CH_3CN$  (80 ml) was stirred for 30 min at RT. 4-acetamido- $\alpha$ -bromopropiophenone (2.43 g, 9.02 mmol) was first dissolved in 40 ml of  $CH_3CN$ , and immediately added dropwise to the reaction mixture over 30 min, [reaction monitored by TLC:  $CH_2Cl_2/CH_3OH$ , 9:1]. After 24 h, the reaction was stopped and poured into ethyl acetate (200 ml). The organic layer was washed three times with a dilute hydrochloric acid water solution (pH=2), dried over  $Na_2SO_4$ , and evaporated to dryness to give a pale-yellow solid compound (6.0 g). A 370.8 mg aliquot of residue product was purified by flash chromatography on silica gel using  $CH_2Cl_2/CH_3OH$  (9:1) as mobile phase. After evaporation of the solvent, 241 mg (2.4 g, 65.0 % of yield) of 4 was obtained as a pale-yellow powder. ESI MS:  $m/z$  726  $[M + Na]^+$ ;  $^1H$  NMR (500 MHz,  $CDCl_3$ , 25 °C, TMS):  $\delta$  1.04 [9H, s,  $C(CH_3)_3$ ], 1.35 [9H, s,  $C(CH_3)_3$ ], 1.26-1.27 (3H, d,  $NCHCH_3$ ,  $J = 7$  Hz), 1.48 [9H, s,  $C(CH_3)_3$ ], 2.06 (3H, s,  $COCH_3$ ), 1.90-3.76 (22H, br m,  $3 \times NCH_2COOH$ ,  $4 \times CH_2NCH_2$ ), 4.54-4.55 (1H, q,  $NCHCH_3$ ,  $J = 10$  Hz), 7.57-7.80 (4H, 2 d,  $ArH$ ,  $J = 10$  Hz), 7.84 (1H, s,  $NHCO$ ).  $^{13}C$  NMR (500 MHz,  $CDCl_3$ , 25 °C, TMS):  $\delta$  11.26, 24.13, 28.35, 28.44, 28.47, 46.67, 53.93, 54.26, 54.66, 56.58, 56.66, 57.12, 60.11, 82.90, 83.00, 83.04, 120.03, 131.10, 132.47, 144.47, 171.96, 174.41, 174.50, 175.21, 204.61.

**Synthesis of 10[2(1-oxo-1-*p*-aminophenyl propyl)]-1,4,7,10-tetraaza cyclodecane-1,4,7-tetraacetic acid (DO3A-APP) (5)**

Two routes of synthesis were used to prepare compound 10[2(1-oxo-1-*p*-aminophenyl propyl)]-1,4,7,10-tetraazacyclodecane-1,4,7-tetraacetic acid (DO3A-APP) (5).

**Route1:** Into a microwave reaction vials, 10[2(1-oxo-1-*p*-acetamidophenyl propyl)]-1,4,7,10-tetraazacyclodecane-1,4,7-tris(acetic acid *t*-butyl ester) (4) (1.0 g, 1.42 mmol) was dissolved in a mixture of 0.1M HCl (7 ml) standard aqueous solution, and 3 ml of HPLC-grade  $CH_3CN$  in order to have a better homogeneous reaction mixture. The reactants were subjected to microwave radiation for 30 min. at 100 °C. The final product was first neutralised at pH=6.8 by using a standard aqueous NaOH (0.1 M) solution, then washed two times with ethyl ether, and dried under rotary evaporator. In order to remove the NaCl salt from the final product, the water solution was dialysed for 7 days by using a membrane with a molecular weight cut-off of 150-300 Da, and freeze-dried to give a pure pale-yellow solid compound 5 (0.582 g, 83% of yield).

**Route 2:** Into a round bottom flask, 10[2(1-oxo-1-*p*-acetamidophenyl propyl)]-1,4,7,10-tetraazacyclodecane-1,4,7-tris(acetic acid *t*-butyl ester) (**4**) (3.922 g, 5.57 mmol) was dissolved in a mixture of 0.1M HCl (25 ml) standard aqueous solution, and 10 ml of HPLC-grade CH<sub>3</sub>CN in order to have a better homogeneous reaction mix. Reaction was stirred under reflux for 4h. The final product was first neutralised at pH=6.8 by using a standard aqueous NaOH (0.1 M) solution, then washed two times with ethyl ether, dried under rotary evaporator first, and then freeze-dried to give a pale-yellow solid compound (3.229 g). In order to remove the NaCl salt from the final product, a 100 mg aliquot of residue product was dialysed for 7 days by using a membrane with a molecular weight cut-off of 150-300 Da, and freeze-dried to give a pure pale-yellow solid compound **5** (0.064 g, 71% of yield). ESI MS: *m/z* 494 [M + H]<sup>+</sup>; <sup>1</sup>H NMR (500 MHz, DMSO-d<sub>6</sub>, 25 °C, TMS): δ 1.22-1.23 (3H, d, NCHCH<sub>3</sub>, J = 7 Hz), 2.90–3.83 (22H, br m, 3xNCH<sub>2</sub>COOH, 4xCH<sub>2</sub>NCH<sub>2</sub>), 4.82 (1H, q, NCHCH<sub>3</sub>, J = 10 Hz), 6.66-7.66 (4H, 2 d, ArH, J = 10 Hz). <sup>13</sup>C NMR (500 MHz, DMSO-d<sub>6</sub>, 25 °C, TMS): δ 14.70, 44.20, 45.49, 48.67, 50.52, 52.17, 55.93, 57.26, 58.66, 59.58, 60.66, 62.12, 64.11, 114.49, 125.19, 131.10, 153.47, 169.41, 170.50, 177.21, 202.61.

***Synthesis of 10[2(1-oxo-1-*p*-isothiocyanophenyl propyl)]-1,4,7,10-tetraazacyclodecane-1,4,7- tetraacetic acid (DO3A-NCSPP) (6)***

DO3A-APP (**5**) (0.582 g, 1.18 mmol) was dissolved in water (10 ml), and the pH was adjusted to 2 by several drops of concentrated HCl aqueous solution. A mixture of thiophosgene (0.170 g, 1.47 mmol, 1.2 equiv.) and 5ml of CCl<sub>4</sub> was added in one portion, and the reaction was vigorously stirred at room temperature for 48 h. The excess of thiophosgene was removed by washing the aqueous mixture, using first CH<sub>2</sub>Cl<sub>2</sub> (3 times) and later ethyl ether (3 times). The water fraction was separated and freeze-dried to get a pale-yellow solid compound (**6**). (0.560 g, 89% of yield). ESI MS: *m/z* 536 [M + H]<sup>+</sup>; <sup>1</sup>H NMR (500 MHz, DMSO-d<sub>6</sub>, 25 °C, TMS): δ 1.37-1.38 (3H, d, NCHCH<sub>3</sub>, J = 7 Hz), 3.06–3.91 (22H, br m, 3xNCH<sub>2</sub>COOH, 4xCH<sub>2</sub>NCH<sub>2</sub>), 4.88-4.93 (1H, q, NCHCH<sub>3</sub>, J = 10 Hz), 6.83-7.80 (4H, 2 d, ArH, J = 10 Hz). <sup>13</sup>C NMR (500 MHz, DMSO-d<sub>6</sub>, 25 °C, TMS): δ 14.40, 48.67, 55.93, 57.26, 58.66, 59.58, 60.66, 62.12, 64.11, 120.03, 131.10, 132.47, 136.52, 144.47, 175.41, 175.50, 176.21, 205.61.



**Synthesis of 10[2(1-oxo-1-p-propylthioureidophenyl propyl)]-1,4,7,10-tetraazacyclodecane-1,4,7-tetraacetic acid ( $L_1$ )**

Propylamine (0.012 g, 0.2 mmol) was dissolved in water (5ml), and the pH was adjusted to 9-10 with diluted NaOH aqueous solution. DO3A-NCSP (6) freshly prepared (0.08 g, 0.15 mmol), was added, and the reaction mixture was stirred at room temperature for 24 h. The crude product (0.16 g) was purified by flash-chromatography (RP-C18 column) with AcN/H<sub>2</sub>O (8:2) as mobile phase, yielding 89% of pure pale-yellow  $L_1$  solid (0.08 g). ESI MS:  $m/z$  595 [ $M+H$ ]<sup>+</sup>; <sup>1</sup>H NMR (500 MHz, D<sub>2</sub>O, 25 °C):  $\delta$  0.73-0.81 (3H, br m, CH<sub>3</sub>CH<sub>2</sub>CH<sub>2</sub>), 1.18-1.19 (3H, d, NCHCH<sub>3</sub>, J = 7 Hz), 1.39-1.49 (2H, br m, CH<sub>3</sub>CH<sub>2</sub>CH<sub>2</sub>), 2.71-3.90 (24H, br m, 3xNCH<sub>2</sub>COOH, 4xCH<sub>2</sub>NCH<sub>2</sub>, CSNHCH<sub>2</sub>CH<sub>2</sub>CH<sub>3</sub>), 4.73-4.81 (1H, q, NCHCH<sub>3</sub>, J = 10 Hz), 7.23-7.76 (4H, 2 d, ArH, J = 10 Hz).

**Synthesis of conjugated API-( $L_1$ )<sub>x</sub> ligand**

The O-(Aminopropyl)inulin (API) sample with degree of substitution (ds) of 0.9 was synthesized from inulin (dp = 32) by following a procedure described previously<sup>[12]</sup>. API (0.245 g, 1.12 mmol amino groups), was dissolved in water (25 ml), and the pH was adjusted to 9-10 with diluted NaOH. DO3A-NCSP (6) freshly prepared (0.757 g, 1.41 mmol), was added to the reaction mixture. The reaction was stopped after 4 days, and purified by ultrafiltration using a membrane with a molecular weight cut-off of 3 kDa. The product was freeze-dried, resulting in 0.6 g of API-( $L_1$ )<sub>x</sub> as a yellow powder. <sup>1</sup>H NMR (500 MHz, D<sub>2</sub>O, 25 °C):  $\delta$  1.20 (br s, NCHCH<sub>3</sub>), 1.80 (br s, CH<sub>2</sub>CH<sub>2</sub>NH<sub>2</sub>), 2.8-3.0 (br m, CH<sub>2</sub>CH<sub>2</sub>NH<sub>2</sub>), 3.1-3.3 (br m, NCH<sub>2</sub>CH<sub>2</sub>N), 3.3-3.6 (br m, NCH<sub>2</sub>COOH), 4.14 (1H, br m, NCHCH<sub>3</sub>), 4.77 (inulin H, br m), 7.35 and 7.74 (4H, 2 br d, ArH). Comparison between integrals of the aromatic protons and those of the sugar protons indicated an averaged ds of 0.9.

**Preparation of (Gd $L_1$ ) and API-(Gd $L_1$ )<sub>x</sub> complexes**

Gd $L_1$  and API-(Gd $L_1$ )<sub>x</sub> complexes were prepared by a stepwise addition of GdCl<sub>3</sub>·6H<sub>2</sub>O to a solution of 80 mg of  $L_1$  (0.13 mmol) and 200 mg of API-( $L_1$ )<sub>x</sub> respectively, in 8 ml of H<sub>2</sub>O, maintaining the pH between 6.5 and 7.0 by addition of 1 M NaOH aqueous solution. After 4 days the reaction mixture was stopped, and the excess of free lanthanide for the Gd $L_1$  complex was removed by centrifugation as Gd(OH)<sub>3</sub> precipitate, which appeared at pH 10 after addition of 1 M NaOH, whereas

for **API-(GdL<sub>1</sub>)x** complex the excess of free gadolinium was removed by ultra-filtration using a membrane with a cut-off of 3 kDa. The absence of free Gd<sup>3+</sup> ions was confirmed by a xylenol orange test, with a final pH of both solutions around 6.5-7.00. The solutions were freeze-dried to give a pale-yellow solid for both final complexes: **GdL<sub>1</sub>** 72 mg, ESI MS: *m/z* 771 [M + Na]<sup>+</sup>; and 0.23 g **API-(GdL<sub>1</sub>)x**.

### NMRD profiles

$1/T_1$  <sup>1</sup>H NMRD profiles were measured on a Stelar Spinmaster FFC fast field cycling NMR relaxometer (Stelar, Mede, Pavia, Italy) over a range of magnetic fields extending from 0.24 mT to 0.7 T and corresponding to <sup>1</sup>H Larmor frequencies from 0.01 to 30 MHz using 0.6 ml samples in 10 mm o.d. tubes. The samples were prepared by dissolution of appropriate amounts of freeze-dried complexes of **GdL<sub>1</sub>** and **API-(GdL<sub>1</sub>)x** in Milli-Q water with the pH in the range 6.5-7.0. The exact Gd<sup>3+</sup> concentration was determined by proton relaxivity measurements at 20 MHz and 37 °C after complete hydrolysis in concentrated HNO<sub>3</sub>. Additional relaxation rates at 20 and 60 MHz were obtained with Bruker Minispec mq-20 and mq-60 spectrometers (Bruker, Karlsruhe, Germany), respectively. The 300 MHz data were obtained on a Bruker Avance-300 high resolution spectrometer.

Fitting of the <sup>1</sup>H NMRD was performed with data processing software that uses different theoretical models describing observed nuclear relaxation phenomena (Mintfit, CERN Library).<sup>[39,40]</sup> The theoretical model takes into account the inner-sphere interaction, the outer-sphere interaction and when necessary the second sphere contribution.<sup>[6]</sup> It has to be noted that, as the macromolecular complex API-(GdL<sub>1</sub>)x is a mixture of different compounds characterized by an averaged *ds* of 0.9, the different parameters extracted from the fitting procedure for this complex are obtained as an average for the mixture of compounds.

### <sup>17</sup>O NMR studies

<sup>17</sup>O NMR relaxation rate measurements were performed on a Bruker Avance II-500 spectrometer using 5 mm diameter sample tubes containing 325 µl (pH 6.5-7.00) of **GdL<sub>1</sub>** (6.81 mM) and **API-(GdL<sub>1</sub>)x** (14.24 mM) solutions. The temperature was regulated by air or N<sub>2</sub> flow controlled by a BVT-3200 unit. <sup>17</sup>O transverse relaxation times of pure water (diamagnetic contribution) were measured using a CPMG sequence and a subsequent two-parameter fit of the data points. The 90 and 180°

pulse lengths were 27.5 and 55  $\mu$ s, respectively. Broadband proton decoupling was applied during the acquisition of all  $^{17}\text{O}$  NMR spectra.  $^{17}\text{O}$   $T_2$  of water in complex solution was obtained from line width measurement. The data are presented as the reduced transverse relaxation rate  $1/T_2^R = 55:55/([\text{Gd complex}] \cdot q \cdot T_2^P)$ , where  $[\text{Gd complex}]$  is the molar concentration of the complex,  $q$  is the number of coordinated water molecules and  $T_2^P$  is the paramagnetic transverse relaxation rate obtained after subtraction of the diamagnetic contribution from the observed relaxation rate. The treatment of the experimental data was performed as already described.<sup>[24,26,50]</sup> It has to be noted that, as the macromolecular complex API-(GdL<sub>1</sub>)<sub>x</sub> is a mixture of different compounds characterized by an averaged ds of 0.9, the  $\tau_M$  value for this complex is obtained as an average for the mixture of compounds.

### Transmetallation

The stability of the monomeric **GdL<sub>1</sub>** complex was determined by a transmetallation method monitoring the  $^1\text{H}$  longitudinal relaxation rates of water during 5 days at 37°C.<sup>[42]</sup> The measurements were performed on a Bruker Minispec mq-20 spin analyzer at 20 MHz using 7 mm sample tubes containing 2.5 mM of Gd<sup>3+</sup>-complex and 2.5 mM of ZnCl<sub>2</sub> in 300  $\mu$ l of phosphate buffer solution (26 mM KH<sub>2</sub>PO<sub>4</sub>, 41 mM Na<sub>2</sub>HPO<sub>4</sub>, pH = 7).

### Acknowledgements

This work was supported by the Walloon Region (program First spin-off), the FNRS (*Fond National de la Recherche Scientifique*), the UIAP VII, ARC Programs of the French Community of Belgium, the FEDER, the Walloon Region (Holocancer and Gadolymph programs), Interreg and the COST Actions (TD 1004, TD1402 and CA15209). The authors thank the Center for Microscopy and Molecular Imaging (CMMI, supported by the European Regional Development Fund and the Walloon Region).

## Author Contribution

The contributions of the respective authors are as follows: Luigi Granato performed the syntheses and the physico-chemical characterization of the different compounds; Luce Vander Elst executed the 17-oxygen NMR analysis and the NMRD profiles; Celine Henoumont interpreted data and revised the manuscript; Robert N. Muller and Sophie Laurent revised the manuscript and supervised the work. All authors read and approved the manuscript.

## References

- [1] R.B. Lauffer, "Paramagnetic Metal Complexes as Water Proton Relaxation Agents for NMR Imaging: Theory and Design", *Chem. Rev.* **1987**, 87, 901-927.
- [2] E. Toth, L. Helm, A.E. Merbach. "Relaxivity of MRI Contrast Agents", in Topics in Current Chemistry. Contrast Agents I; Springer, Berlin 2002, 221,p. 61–101.
- [3] C.F. Geraldes, S. Laurent, "Classification and basic properties of contrast agents for magnetic resonance imaging". *Contrast Media Mol. Imaging* **2009**, 4(1), 1-23.
- [4] P. Caravan, J.J. Ellison, T.J. McMurry, R.B. Lauffer, "Gadolinium(III) chelates as MRI contrast agents: Structure, Dynamics, and Applications", *Chem. Rev.* **1999**, 99, 2293-2352.
- [5] S. Aime, M. Botta, E. Terreno, "Gd(III)-Based Contrast Agents for MRI", *Adv. Inorg. Chem. Eur. J.* **2005**, 57, 173-237.
- [6] A.S. Merbach, L. Helm, E. Tóth, "The Chemistry of Contrast Agents in Medical Magnetic Resonance Imaging", Second Edition. *John Wiley & Sons* 2013.
- [7] N. Bloembergen, "Proton Relaxation Times in Paramagnetic Solutions". *J. Chem. Phys.* **1957**, 27, 572.
- [8] N. Bloembergen, L.O. Morgan, "Proton relaxation times in paramagnetic solutions: effects of electron spin relaxation", *J. Chem. Phys.* **1961**, 34, 842-850.

- [9] E. Strandberg, P.O. Westlund, "<sup>1</sup>H NMRD Profile and ESR Lineshape Calculation for an Isotropic Electron Spin System with S= 7/2. A Generalized Modified Solomon–Bloembergen–Morgan Theory for Nonextreme-Narrowing Conditions", *J. Magn. Reson., Ser A* **1996**, 122, 179-191.
- [10] P. Caravan, C.T. Farrar, L. Frullano, R. Uppal, "Influence of molecular parameters and increasing magnetic field strength on relaxivity of gadolinium- and manganese-based  $T_1$  contrast agents", *Contrast Media Mol. Imaging* **2009**, 4, 89-100.
- [11] P. Herman, J. Kotek, V. Kubíček, I. Lukeš. "Gadolinium(III) complexes as MRI contrast agents: ligand design and properties of the complexes". *Dalton Trans* **2008**, 3027-3047.
- [12] L. Granato, S. Laurent, L. Vander Elst, K. Djanashvili, J.A. Peters, R.N. Muller." The Gd<sup>3+</sup> complex of 1,4,7,10-tetraazacyclododecane-1,4,7,10-tetraacetic acid mono(p-isothiocyanatoanilide) conjugated to inulin: a potential stable macromolecular contrast agent for MRI". *Contrast Media Mol. Imaging* **2011**, 6, 482-491.
- [13] C.V. Stevens, A. Meriggi, K. Booten. "Chemical modification of inulin, a valuable renewable resource, and its industrial applications". *Biomacromolecules* **2002**, 1-16.
- [14] A.D. Sherry, Y. Wu. "The importance of water exchange rates in the design of responsive agents for MRI". *Curr. Opin. Chem. Biol.* **2013**, 17, 167-174.
- [15] B.N. Siriwardena-Mahanama, M.J. Allen. "Strategies for optimizing waterexchange rates of lanthanide-based contrast agents for magnetic resonance imaging". *Molecules* **2013**, 18, 9352-9381.
- [16] R. Ruloff, E. Tóth, R. Scopelliti, R. Tripier, H. Handel, A.E. Merbach. "Accelerating water exchange for Gd(III) chelates by steric compression around the water binding site". *Chem. Commun.* **2002**, 2630-2631.
- [17] Z. Jászberényi, A. Sour, E. Tóth, M. Benmelouka, A.E. Merbach. "Fine-tuning water exchange on Gd(III) poly(amino carboxylates) by modulation of steric crowding". *Dalton Trans* **2005**, 2713–2719.
- [18] E. Balogh, R. Tripier, P. Fousková, F. Reviriego, H. Handel, E. Tóth. "Monopropionate analogues of DOTA4- and DTPA5-: Kinetics of formation and dissociation of their lanthanide(III) complexes". *Dalton Trans* **2007**, 3572-3581.

- [19] M.F. Ferreira, A.F. Martins, J.A. Martins, P.M. Ferreira, E. Tóth, C.F.G.C. Geraldes. "Gd(DO3A-N- $\alpha$ -aminopropionate): a versatile and easily available synthon with optimized water exchange for the synthesis of high relaxivity, targeted MRI contrast agents". *Chem. Commun.* **2009**, 6475-6477.
- [20] J.P. André, H.R. Maecke, E. Tóth, A.E. Merbach. "Synthesis and physicochemical characterization of a novel precursor for covalently bound macromolecular MRI contrast agents". *J. Biol. Inorg. Chem.* **1999**, 4, 341-347.
- [21] S. Aime, M. Botta, Z. Garda, B.E. Kucera, G. Tircso, V.G. Young, M. Woods. "Properties, solution state behavior, and crystal structures of chelates of DOTMA". *Inorg. Chem.* **2011** 50(17), 7955-7965.
- [22] S. Zhang, Z. Kovacs, S. Burgess, S. Aime, E. Terreno, A.D. Sherry. "{DOTAbis(amide)}lanthanide complexes: NMR evidence for differences in water-molecule exchange rates for coordination isomers". *Chem. Eur. J.* **2001**, 7, 288-296.
- [23] S. Aime, A. Barge, J.I. Bruce et al. "NMR, relaxometric, and structural studies of the hydration and exchange dynamics of cationic lanthanide complexes of macrocyclic tetraamide ligands". *J. Am. Chem. Soc.* **1999**, 121, 5762-5771.
- [24] S. Laurent, L. Vander Elst, S. Houze, N. Guerit, R.N. Muller. "Synthesis and characterization of various benzyl diethylenetriaminepentaacetic acids (dtpa) and their paramagnetic complexes. Potential contrast agents for magnetic resonance imaging". *Helv Chim Acta* 2000;83:394-406.
- [25] I. Solomon. "Relaxation Processes in a System of Two Spins". *Phys. Rev.* **1955**, 99, 559-565.
- [26] J.H. Freed. "Dynamic effects of pair correlation functions on spin relaxation by translational diffusion in liquids. II. Finite jumps and independent T<sub>1</sub> processes". *J. Chem. Phys.* **1978**, 68, 4034-4037.
- [27] D.H. Powell, O.M. Ni Dhubhghaill, D. Pubanz, L. Helm, Y.S. Lebedev, W. Schlaepfer, A.E. Merbach. "Structural and Dynamic Parameters Obtained from <sup>17</sup>O NMR, EPR, and NMRD Studies of Monomeric and Dimeric Gd<sup>3+</sup> Complexes of Interest in Magnetic Resonance Imaging: An Integrated and Theoretically Self-Consistent Approach". *J. Am. Chem. Soc.* **1996**, 118, 9333-9346.



- [28]. W.P. Cacheris, S.C. Quay, S.M. Rocklage. "The relationship between thermodynamics and the toxicity of gadolinium complexes". *Magn. Reson. Imaging* **1990**, 8(4), 467-481.
- [29] D.H. White, L.A. DeLearie, D.A. Moore, R.A. Wallace, T.J. Dunn, W.P. Cacheris, H. Imura, G.R. Choppin. "The thermodynamics of complexation of lanthanide (III) DTPA-bisamide complexes and their implication for stability and solution structure". *Invest. Radiol.* **1991**, 26, S226-S228.
- [30] C. Paul-Roth, K.N. Raymond. "Amide Functional Group Contribution to the Stability of Gadolinium(III) Complexes: DTPA Derivatives". *Inorg. Chem.* **1995**, 34, 1408-1412.
- [31] S.W.A. Bligh, A.H.M.S. Chowdhury, M. McPartlin et al. "Neutral gadolinium(III) complexes of bulky octadentate dtpa derivatives as potential contrast agents for magnetic resonance imaging". *Polyhedron* **1995**, 14(4), 567-569.
- [32] P.F. Sieving, A.D. Watson, S.M. Rocklage. "Preparation and characterization of paramagnetic polychelates and their protein conjugates". *Bioconjugate Chem.* **1990**, 1, 65-71.
- [33] Y.J. Fu, H.J. Raatschen, D.E. Nitecki, M.F. Wendland, V. Novikov, L.S. Fournier, C. Cyran, V. Rogut, D.M. Shames, R.C. Brasch. "Cascade polymeric MRI contrast media derived from poly(ethylene glycol) cores: initial syntheses and characterizations". *Biomacromolecules* **2007**, 8, 1519-1529.
- [34] P. Caravan, G. Parigi, J.M. Chasse, N.J. Cloutier, J.J. Ellison, R.B. Lauffer, C. Luchinat, S.A. McDermid, M. Spiller, T.J. McMurry. "Albumin binding, relaxivity, and water exchange kinetics of the diastereoisomers of MS-325, a gadolinium(III)-based magnetic resonance angiography contrast agent". *Inorg. Chem.* **2007**, 46, 6632-6639.
- [35] A.J.L. Villaraza, A. Bumb, M.W. Brechbiel. "Macromolecules, dendrimers, and nanomaterials in magnetic resonance imaging: the interplay between size, function, and pharmacokinetics". *Chem. Rev.* **2010**, 110, 2921-2959.
- [36] E. Battistini, E. Gianolio, R. Gref, P. Couvreur, S. Fuzerova, M. Othman, S. Aime, B. Badet, P. Durand. "High-relaxivity magnetic resonance imaging (MRI) contrast agent based on supramolecular assembly between a gadolinium chelate, a modified dextran, and poly-beta-cyclodextrin". *Chem.: A Eur. J.* **2008**, 14, 4551-4561.

- [37] S.H. Medina, M.E.H. El-Sayed. "Dendrimers as carriers for delivery of chemotherapeutic agents". *Chem. Rev.* **2009**, 109, 3141-3157.
- [38] D.L. Verraest, L.P. Da Silva, J.A. Peters, H. Van Bekkum. "Synthesis of cyanoethyl inulin, aminopropyl inulin and carboxyethyl inulin". *Starch-Stärke* **1996**, 48, 191-195.
- [39] R.N. Muller, B. Raduchel, S. Laurent, J. Platzek, C. Pierart, P. Mareski, L. Vander Elst. "Physicochemical characterization of MS-325, a new gadolinium complex, by multinuclear relaxometry". *Eur. J. Inorg. Chem.* **1999**, 1949-1955.
- [40] P. Vallet. "Relaxivity of nitroxide stable free radicals. Evaluation by field cycling method and optimisation". *PhD Thesis, University of Mons* 1992.
- [41] C.M. Alpoim, A.M. Urbano, C.F.G.C. Geraldes, J.A. Peters. "Determination of the number of inner-sphere water molecules in lanthanide (III) Polyaminocarboxylate complexes". *J. Chem. Soc. Dalton Trans* **1992**, 463-467.
- [42] S. Laurent, L. Vander Elst, F. Copoix, R.N. Muller, "Stability of MRI paramagnetic contrast media: a proton relaxometric protocol for transmetallation assessment". *Invest. Radiol.* **2001**, 36(2), 115-122.